

Accepted April 10th 2022

Thermal entrance problem for blood flow inside an axisymmetric tube: The classical Graetz problem extended for Quemada's bio-rheological fluid with axial conduction.

Muhammad Waris Saeed Khan^{*a}, Nasir Ali^a and O. Anwar Bég^b

^{*a}Department of Mathematics and Statistics, International Islamic University, Islamabad 44000, Pakistan

^bProfessor and Director -Multiphysical Engineering Sciences Group (MPESG), Aeronautical and Mechanical Engineering Department, Salford University, UK

*Corresponding author, email: waris.saeed88@gmail.com

Abstract: The heat-conducting nature of blood is critical in the human circulatory system and features also in important thermal regulation and blood processing systems in biomedicine. Motivated by these applications, in the present investigation, the classical Graetz problem in heat transfer is extended to the case of a bio-rheological fluid model. The Quemada bio-rheological fluid model is selected since it has been shown to be accurate in mimicking physiological flows (blood) at different shear rates and hematocrits. The two-dimensional energy equation is tackled via a separation of variables approach for the uniform surface temperature case. Following the introduction of transformation variables, the ensuing dimensionless boundary value problem is solved numerically via **MATLAB** based algorithm known as **Bvp5c** (a finite difference code that implements the four-stage Lobatto IIIa collocation formula). Numerical validation is also presented against two analytical approaches namely, series solutions and Kummer function techniques. Axial conduction in terms of Péclet number is also considered. Typical values of Reynolds number and Prandtl number are used to categorize the vascular regions. The graphical representation of mean temperature, temperature gradient and Nusselt numbers along with detail discussions are presented for the effects of Quemada non-Newtonian parameters and Péclet number. The current analysis may also have potential applications for the development of microfluidic and biofluidic devices particularly which are used in the diagnosis of disease in addition to blood oxygenation technologies.

Key words: Graetz problem, Quemada fluid, Concentrated suspension, S-L boundary value problem, Péclet number, Newton Raphson method, Simpson's rule, Bvp5c.

Nomenclature

ρ	Fluid density
d/dt	Material derivative
r	Radial coordinate
D_h	Hydraulic diameter

\bar{V}	Mean velocity
$V_{N,m}$	Newtonian mean velocity
Pr	Prandtl number
θ_m	Bulk temperature
Nu	Local Nusselt number
τ_{rz}	Shear stress
∇	Gradient operator
T	Temperature
Φ	Viscous dissipation
$\alpha = k/\rho c_p$	Thermal diffusivity
z	Axial coordinate
β^*, q	Quemada rheological parameters
Re_D	Reynolds number
r_0	Half width
λ	Eigenvalue
c_p	Specific heat
k^*	Thermal conductivity
θ	Non-dimensional temperature
Pe	Péclet number
τ	Extra stress tensor
V	Velocity profile
Nu_m	Average Nusselt number
S	Eigenfunction
n	1, 2, 3...

*	Non-dimensional quantities
ΔT	Temperature difference
T_s	Surface temperature
T_i	Inlet temperature

1. Introduction

The non-Newtonian nature of blood as manifested in its shear-thinning and stress relaxation characteristics is well documented. In view of growing evidence that many pathological conditions in the cardiovascular system are influenced in their development and advancement by the flow properties of blood, mathematical and numerical simulation of blood transport phenomena have taken on significant importance [1-3]. The complexity of the blood is due to a non-trivial coupling between constantly moving and deforming red blood cells (RBCs, the majority of blood components) and the fluid carrier. In essence, the movement of blood cells has a strong impact on the global flow of blood, and it is important to understand the movement of cells in various flows and geometries which in turn provides a deeper insight into the elucidation of for example cardiovascular disease (the world's leading cause of death). Recent interest in advancement of membrane oxygenators and extra-corporeal circulation devices has also mobilized interest in for example regulating the temperature of blood. An exact prediction of temperature profile is, therefore, of paramount interest.

The analysis of thermal entry flow phenomenon inside a circular tube in conjunction with hydrodynamically developed velocity is known as the classical Graetz problem. In 1883, *Graetz* [4] studied this problem for slug flow and later, in 1885 for a parabolic flow field. In his analysis he solved the simplified Graetz problem (without axial conduction and dissipation function) with the help of separation of variable method and converted two-dimensional energy equation into an eigenvalue problem. *Nusselt* [5] adopted the same approach of Graetz and refined the analysis elegantly, leading to the Graetz-Nusselt problem. *Siegel et al.* [6] analytically studied the extended Graetz problem for a prescribed heat flux boundary condition. *Hsu* [7-9] presented a detail review of the Graetz problem with axial conduction terms in the energy equation, in which he claimed that the axial conduction term could not be ignored for *Péclet number* < 100 , for which a more accurate heat transfer analysis is required. He also emphasized that as the typical values of *Péclet number* are reduced below 100, one notices that

the calculated eigenvalues and corresponding coefficient of solution series tend to diverge considerably more than those that are obtained for the negligible conduction scenario. In general, as the *Péclet number* is decreased, the magnitude of the corresponding eigenvalues decreases, suggesting that the axial conduction effect becomes increasingly influential as the Peclet number becomes smaller. In fact, when the Péclet number is reduced from 5 to 1 the rate of decrease of the eigenfunctions is seen to be markedly significant. The reduction in the magnitude of the eigenvalues, from a computational point of view, allows further eigenvalues to be determined in order to achieve a converged temperature solution. This is the main reason of calculation of the first fifty eigenvalues in these theoretical study [7-9]. **Shah and London [10]** presented an excellent review of internal flows and heat transfer in ducts with various cross-sections. In recent years, many researchers have extended the Graetz problem to non-Newtonian fluids, owing to significant emerging areas in hemodynamics, chemical engineering, materials processing etc. **Johnston [11]** studied the Graetz problem inside a circular tube for Bingham plastic (yield stress) fluid including the axial conduction term, with an integral transform approach. **Johnston [12]** investigated the Graetz problem for power-law fluids with longitudinal conduction, deriving the temperature profile for both *shear-thinning i. e. pseudoplastic* ($n < 1$) and shear-thickening i. e. *dilatant* ($n > 1$) fluids by employing an integral transform technique. **Lahjomeri et al. [13]** studied the Graetz-Nusselt problem with axial conduction effect and derived analytical expressions for the calculation of eigenfunctions and constants in both upstream and downstream regions with a modified Gram-Schmidt orthonormal procedure. The classical Graetz problem *for viscoelastic effects* was first reported by **Coelho et al. [14]**, who used a simplified PTT fluid model for both a circular tube and a flat channel under imposed surface temperature and prescribed heat flux cases, respectively. Later, **Oliveria et al. [15]** revisited the analysis in [14] for FENE-P fluid model with the same methodology. **Filali et al. [16]** solved the Graetz-Nusselt problem numerically for FENE-P liquids for non-circular (e. g. elliptic) cross-sections using computational fluid dynamics (CFD). Recently, **Ali and Khan [17]** presented an analytical treatment of the Graetz-Nusselt problem for Ellis fluids with both prescribed heat flux and imposed constant wall temperature boundary conditions. Blood flow analysis in entrance regions of both tube and channel confinements was investigated for a Casson viscoplastic fluid with isothermal wall conditions by **Khan and Ali [18]**. **Khan et al. [19]** studied the Graetz problem with a Robertson-Stiff fluid model for both tube and channel geometries again under constant wall temperature boundary condition.

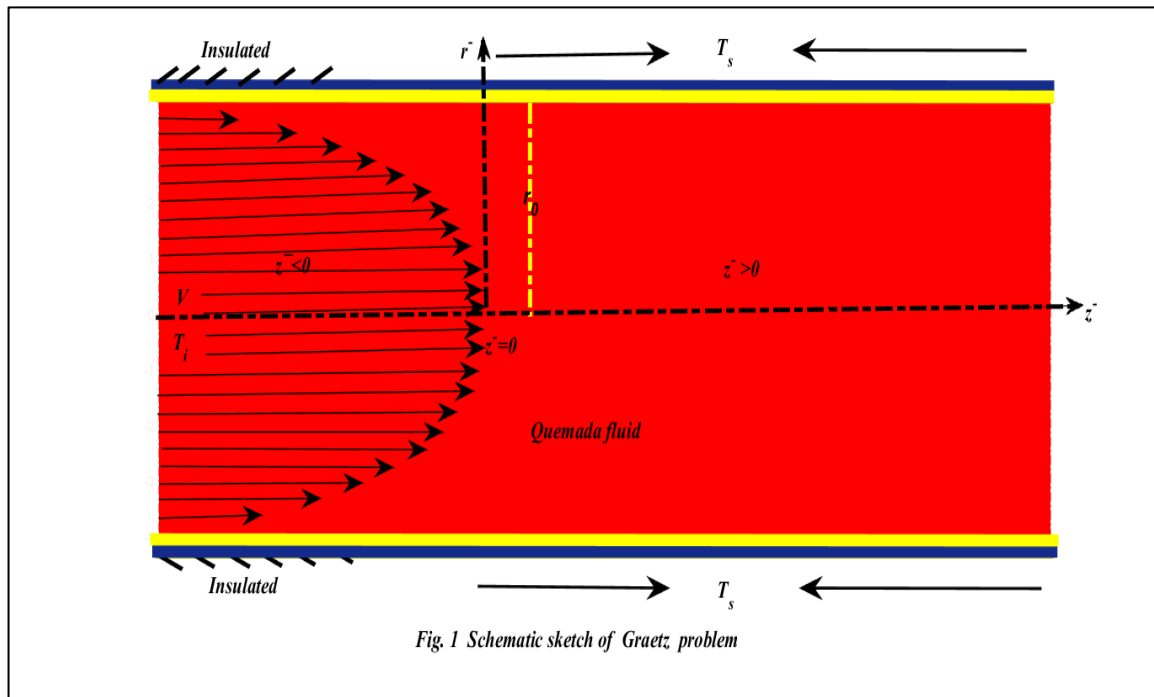
An alternative rheological model to those described thus far, is the *Quemada model* [20] which belongs to the class of generalized Newtonian fluid models. This model successfully predicts the shear-thinning behaviour of physiological liquids e. g. blood. Generally, the Quemada fluid model is based on an intrinsic viscosity which is governed by a *kinetic equation*. In simple shear flows, the intrinsic viscosity becomes a function of the local shear rate and suspension of particles. This fluid model basically is an extension of Casson's viscoplastic (yield stress) fluid model but contains three parameters. This model explicitly describes also the kinetics of RBC aggregation and approximates the bulk rheology of real blood quite well. The viscosity is not infinite at zero shear rates in the Quemada model and it is therefore also popular for analysing blood flow in microvessels. Furthermore, it accurately fits experimental viscometric data for small diameter vessels (above 12 μ m diameter) as noted in Das *et al.* [21]. The Quemada viscosity results for this model fall in the range between in vitro and in vivo values and it is a robust approach for modelling RBC suspensions. It is therefore one of the very best hemorheological models since it is in excellent agreement with experimental observations. The applications of this fluid model are quite broad and relevant studies include [22]-[25] in a range of clinical situations. However very few studies have presented analytical solution for velocity field and mean flow rate. From an inspection of the literature, no work has so far been reported on the Graetz problem for a Quemada fluid. This is therefore the focus of the current study. Practically this problem models the *thermal entrance flow of blood in a circular tube*. Moreover, the axial conduction effects for three vascular regions, namely, core vascular, subcutaneous vascular and microvascular regions are also taken into account.

In order to address in detail, the effects of non-Newtonian Quemada fluid characteristics on the heat transfer properties, the remainder of this article is categorized as follows. The analytical expression for velocity profile, a schematic sketch of flow problem and formulation of energy equation and the corresponding solution are reported in *section 2*. Validation of numerical results with analytical approaches is presented in *section 3*. The detailed discussions through graphs and tables are provided in *section 4*. Lastly, some conclusions are drawn in *section 5*.

2. Mathematical Model

Consider the entry flow of Quemada bio-rheological fluid in a duct with circular cross-section with a hydrodynamically developed velocity field and specified inlet temperature (T_i) as displayed in **Fig. 1**. The tube wall is specified at imposed uniform surface temperature (T_s).

The objective is to compute the thermally developing temperature field in term of Nusselt number for Quemada bio-rheological fluid *with axial conduction*.



For this analysis, we shall apply the basic conservation laws as given below.

$$\nabla \cdot \mathbf{V} = 0, \quad (\text{Continuity equation}) \quad (1)$$

$$\rho \frac{d\mathbf{V}}{dt} = -\nabla P + \nabla \cdot \boldsymbol{\tau}, \quad (\text{Momentum equation}) \quad (2)$$

$$\rho c_p \frac{dT}{dt} = k \nabla^2 T + \phi, \quad (\text{Energy equation}) \quad (3)$$

The constitutive relation for Quemada bio-rheological fluid is [26]:

$$\sqrt{\tau_{rz}} = \left[\sqrt{\eta_\infty} + \frac{\sqrt{\tau_0}}{\sqrt{\sigma} + \sqrt{\dot{\gamma}}} \right] \sqrt{\dot{\gamma}}, \quad (4)$$

where η_∞ , σ and τ_0 are expressed as

$$\eta_\infty = \frac{\eta_p}{\left(1 - \frac{1}{2} k_\infty H\right)^2}, \quad (5)$$

$$\sigma = \gamma_c \left(\frac{1 - \frac{1}{2} k_0 H}{1 - \frac{1}{2} k_\infty H} \right)^2, \quad (6)$$

$$\tau_0 = \eta_p \gamma_c \frac{\left(\frac{1}{2} H (k_0 - k_\infty) \right)^2}{\left(1 - \frac{1}{2} k_\infty H \right)^4}. \quad (7)$$

In the above equation H is particle (e. g. red blood cell) concentration and k_0, k_∞, γ_c are Quemada parameters respectively. It is important to mention that when we take $\sigma \rightarrow 0$ in Eqn. (4) then it reduces to Casson bio-rheological fluid model. For simple shear flow, the z -component of momentum equation can be expressed as a linear function of r .

$$\tau_{rz} = P \frac{r}{2}, \quad (8)$$

where

$$P = \frac{(p_{in} - p_{out})}{L}. \quad (9)$$

In Eq. (9) p_{in} is the inlet pressure, p_{out} denotes the outlet pressure and L is the tube (blood vessel) length. Beside that the shear stress at the wall is $\tau_w = P r_0 / 2$ and $\dot{\gamma} = \left| \frac{dV}{dr} \right|$. Now introducing the following dimensionless parameters:

$$\bar{r} = \frac{r}{r_0}, \quad \beta^* = \frac{\sqrt{\tau_0} + \sqrt{\eta_\infty \sigma}}{\sqrt{\tau_w}}, \quad q = \frac{\sqrt{\tau_0} - \sqrt{\eta_\infty \sigma}}{\sqrt{\tau_0} + \sqrt{\eta_\infty \sigma}}, \quad \bar{z} = \frac{z}{R_{eD} Pr D_h}, \quad R_{eD} = \frac{V_m D_h}{\nu}, \quad \theta = \frac{T - T_s}{\Delta T},$$

$$P\bar{e} = 2R_{eD} Pr \quad (10)$$

Using Eqn. (10) into Eqn. (4) the expression for shear stress can be presented as:

$$\left| \dot{\gamma} \right| = -\frac{dV}{dr} = \frac{Pr_0}{4\eta_\infty} \left[\bar{r} - \beta^* (1+q) \sqrt{\bar{r}} + \beta^{*2} + (\sqrt{\bar{r}} - \beta^*) \sqrt{\bar{r} - 2\beta^* q \sqrt{\bar{r}} + \beta^{*2}} \right] \quad (11)$$

The final expression for velocity field satisfying the condition $V(1) = 0$ can be read as [27]

$$\begin{aligned}
V = & \frac{Pr_0^2}{4\eta_\infty} \left[\frac{1}{2} \left[(1-\beta^*q)^4 - (\sqrt{\bar{r}} - \beta^*q)^4 \right] + \frac{2}{3} \beta^* (2q-1) \left[(1-\beta^*q)^3 - (\sqrt{\bar{r}} - \beta^*q)^3 \right] + \beta^{*2} (q-1)^2 \right. \\
& \left[(1-\beta^*q)^2 - (\sqrt{\bar{r}} - \beta^*q)^2 \right] - 2\beta^{*3} q (q-1) (1-\sqrt{\bar{r}}) + \frac{1}{2} \left\{ \left(1 + \frac{1}{3} \beta^* (5q-4) \right) (1-2\beta^*q + \beta^{*2})^{\frac{3}{2}} \right. \\
& \left. - \left(\sqrt{\bar{r}} + \frac{1}{3} \beta^* (5q-4) \right) (\bar{r} - 2\beta^*q\sqrt{\bar{r}} + \beta^{*2})^{\frac{3}{2}} \right\} + \frac{1}{4} \beta^{*2} (q-1) (5q+1) \left[(1-\beta^*q)(1-2\beta^*q + \beta^{*2})^{\frac{1}{2}} \right. \\
& \left. - (\sqrt{\bar{r}} - \beta^*q)(\bar{r} - 2\beta^*q\sqrt{\bar{r}} + \beta^{*2})^{\frac{1}{2}} - (\sqrt{\bar{r}} - \beta^*q)(\bar{r} - 2\beta^*q\sqrt{\bar{r}} + \beta^{*2})^{\frac{1}{2}} \right] - \frac{1}{4} \beta^{*4} (q-1)^2 (q+1) \\
& \left. (5q+1) \ln \left[\frac{(1-2\beta^*q + \beta^{*2})^{\frac{1}{2}} + 1 - \beta^*q}{(\bar{r} - 2\beta^*q\sqrt{\bar{r}} + \beta^{*2})^{\frac{1}{2}} + \sqrt{\bar{r}} - \beta^*q} \right] \right], \quad 0 \leq \bar{r} \leq 1. \quad (12)
\end{aligned}$$

The parameters β^* and q must satisfy the condition $\beta^* > 0$ and $-1 \leq q \leq 1$. It is important to note that Eqn. (12) represents the velocity for *Hagen-Poiseuille flow* of Casson bio-rheological fluid in a tube for $q=1$ i.e., $\sigma \rightarrow 0$ while it reduces to *the* Newtonian fluid velocity profile for $q=-1$ and $\beta^* = 0$. The mean velocity can be calculated using the following relation [27]:

$$V_m = \frac{2\pi}{\pi r_0^2} \int_0^{r_0} r V dr = \frac{r_0}{\tau_w^3} \int_0^{\tau_w} \tau_{rz}^2 f(\tau) d\tau, \quad (13)$$

where $\dot{\gamma} = f(\tau)$.

Employing (13), we get:

$$V_m = \frac{Pr_0^2}{8\eta_\infty} [F(\beta^*, q)] \quad (14)$$

$$F(\beta^*, q) = \frac{1}{2} \left[\begin{aligned} & 1 - \frac{8}{7} \beta^* (1+q) + \frac{4}{3} \beta^{*2} - \beta^{*8} A_7 + \left(1 + \sum_{n=1}^7 \beta^{*n} A_n \right) \sqrt{1 - 2\beta^*q + \beta^{*2}} + \\ & \beta^{*8} A_8 \ln \frac{1 - \beta^*q + \sqrt{1 - 2\beta^*q + \beta^{*2}}}{\beta^* (1-q)} \end{aligned} \right], \quad (15)$$

where A_i , $i=1-8$ are polynomials in terms of q and are listed in Appendix 1. When $q \rightarrow 1$, Eqn. (15) reduces to the expression for the *mean velocity* of a Casson bio-rheological fluid which is given by:

$$V_m = \frac{Pr_0^2}{8\eta_\infty} \left[1 - \frac{16}{7} \beta^* + \frac{4}{3} \beta^{*2} - \frac{1}{21} \beta^{*8} \right] \quad \text{with } \beta^* = \left(\frac{\tau_0}{\tau_w} \right)^{\frac{1}{2}} \quad (16)$$

The *non-dimensional* energy equation needed for thermal analysis may be written as:

$$\bar{U}(\bar{r}) \frac{\partial \theta(\bar{z}, \bar{r})}{\partial \bar{z}} = 4 \left(\frac{\partial^2 \theta(\bar{z}, \bar{r})}{\partial \bar{r}^2} + \frac{1}{\bar{r}} \frac{\partial \theta(\bar{z}, \bar{r})}{\partial \bar{r}} + \frac{1}{Pe^2} \frac{\partial^2 \theta(\bar{z}, \bar{r})}{\partial \bar{z}^2} \right), \quad (17)$$

where $\bar{U} = V/V_{N,m}$ and $V_{N,m}$ represents the Newtonian mean velocity. The non-dimensional boundary conditions for the constant temperature case are:

$$\left. \begin{array}{l} \theta(0, \bar{r}) = 1 \\ \theta(\bar{z}, 1) = 0 \\ \frac{\partial \theta(\bar{z}, 0)}{\partial \bar{r}} = 0 \end{array} \right\}. \quad (18)$$

The solution of the *elliptic* energy equation is obtained with the famous *separation of variable approach*. The resulting equations and the boundary condition after substituting the separable relation $\theta(\bar{r}, \bar{z}) = S(\bar{r})N(\bar{z})$ into Eqns. (17) and (18) then read:

$$\frac{dN}{d\bar{z}} + 2\lambda_n^2 N = 0, \quad (19)$$

$$\begin{aligned} & S''(\bar{r}) + \frac{1}{\bar{r}} S'(\bar{r}) + \lambda_n^2 \\ & \left[\frac{\lambda_n^2}{Pe^2} \pm \left[\frac{1}{2} \left[(1 - \beta^* q)^4 - (\sqrt{\bar{r}} - \beta^* q)^4 \right] + \frac{2}{3} \beta^* (2q - 1) \left[(1 - \beta^* q)^3 - (\sqrt{\bar{r}} - \beta^* q)^3 \right] + \beta^{*2} (q - 1)^2 \right. \right. \\ & \left. \left[(1 - \beta^* q)^2 - (\sqrt{\bar{r}} - \beta^* q)^2 \right] - 2\beta^{*3} q (q - 1) (1 - \sqrt{\bar{r}}) + \frac{1}{2} \left\{ \left(1 + \frac{1}{3} \beta^* (5q - 4) \right) (1 - 2\beta^* q + \beta^{*2})^{\frac{3}{2}} \right. \right. \\ & \left. \left. - \left(\sqrt{\bar{r}} + \frac{1}{3} \beta^* (5q - 4) \right) (\bar{r} - 2\beta^* q \sqrt{\bar{r}} + \beta^{*2})^{\frac{3}{2}} \right\} + \frac{1}{4} \beta^{*2} (q - 1) (5q + 1) \left[(1 - \beta^* q) (1 - 2\beta^* q + \beta^{*2})^{\frac{1}{2}} \right. \right. \\ & \left. \left. - (\sqrt{\bar{r}} - \beta^* q) (\bar{r} - 2\beta^* q \sqrt{\bar{r}} + \beta^{*2})^{\frac{1}{2}} - (\sqrt{\bar{r}} - \beta^* q) (\bar{r} - 2\beta^* q \sqrt{\bar{r}} + \beta^{*2})^{\frac{1}{2}} \right] - \frac{1}{4} \beta^{*4} (q - 1)^2 (q + 1) \right. \\ & \left. \left. (5q + 1) \ln \left[\frac{(1 - 2\beta^* q + \beta^{*2})^{\frac{1}{2}} + 1 - \beta^* q}{(\bar{r} - 2\beta^* q \sqrt{\bar{r}} + \beta^{*2})^{\frac{1}{2}} + \sqrt{\bar{r}} - \beta^* q} \right] \right] \right] S(\bar{r}) = 0 \end{aligned} \quad (20)$$

$$\left. \begin{array}{l} S'(0) = 0 \\ S(1) = 0 \end{array} \right\}. \quad (21)$$

Eqn. (20) is not a regular Sturm-Liouville boundary value problem (SLBVP) – see Kreyzig [28] - and therefore, the eigenfunctions *are not orthogonal* with respect to the following weighting function:

$$\begin{aligned}
& \left[\frac{1}{2} \left[(1 - \beta^* q)^4 - (\sqrt{\bar{r}} - \beta^* q)^4 \right] + \frac{2}{3} \beta^* (2q - 1) \left[(1 - \beta^* q)^3 - (\sqrt{\bar{r}} - \beta^* q)^3 \right] + \beta^{*2} (q - 1)^2 \right. \\
& \left[(1 - \beta^* q)^2 - (\sqrt{\bar{r}} - \beta^* q)^2 \right] - 2\beta^{*3} q (q - 1) (1 - \sqrt{\bar{r}}) + \frac{1}{2} \left\{ \left(1 + \frac{1}{3} \beta^* (5q - 4) \right) (1 - 2\beta^* q + \beta^{*2})^{\frac{3}{2}} \right. \\
& \left. - \left(\sqrt{\bar{r}} + \frac{1}{3} \beta^* (5q - 4) \right) (\bar{r} - 2\beta^* q \sqrt{\bar{r}} + \beta^{*2})^{\frac{3}{2}} \right\} + \frac{1}{4} \beta^{*2} (q - 1) (5q + 1) \left[(1 - \beta^* q) (1 - 2\beta^* q + \beta^{*2})^{\frac{1}{2}} \right. \\
& \left. - (\sqrt{\bar{r}} - \beta^* q) (\bar{r} - 2\beta^* q \sqrt{\bar{r}} + \beta^{*2})^{\frac{1}{2}} - (\sqrt{\bar{r}} - \beta^* q) (\bar{r} - 2\beta^* q \sqrt{\bar{r}} + \beta^{*2})^{\frac{1}{2}} \right] - \frac{1}{4} \beta^{*4} (q - 1)^2 (q + 1) \\
& \left. (5q + 1) \ln \left[\frac{(1 - 2\beta^* q + \beta^{*2})^{\frac{1}{2}} + 1 - \beta^* q}{(\bar{r} - 2\beta^* q \sqrt{\bar{r}} + \beta^{*2})^{\frac{1}{2}} + \sqrt{\bar{r}} - \beta^* q} \right] \right] \quad (22)
\end{aligned}$$

To overcome this difficulty, we first employ the Bvp5c algorithm available in MATLAB symbolic software for the solution of Eqn. (20) in terms of the eigenvalues λ_n and the related eigenfunctions $S_n(\bar{r})$. Next, a modified Gram Schmidt process [29, 30] is implemented for computation of the coefficients of the solution series and is given by:

$$\theta = \sum_0^n D_n S_n(\bar{r}) \exp(-2\lambda_n^2 \bar{z}). \quad (23)$$

The integrals arising in the computation of D_n are determined via Simpson's rule. The average temperature and Nusselt numbers can be achieved by employing the following relations.

$$\theta_m(\bar{z}) = \frac{\int_0^1 \bar{U} \theta(\bar{r}, \bar{z}) \bar{r} d\bar{r}}{\int_0^1 \bar{U} \bar{r} d\bar{r}}, \quad (24)$$

$$Nu(\bar{z}) = \frac{(-2)}{\theta_m(\bar{z})} \frac{\partial \theta(\bar{z}, 1)}{\partial \bar{r}}, \quad (25)$$

$$Nu_m(\bar{z}) = \frac{1}{\bar{z}} \int_0^{\bar{z}} Nu(\bar{z}) d\bar{z}. \quad (26)$$

3. Test case for Numerical algorithm

It is remarked that an analytical solution of Eqn. (17) is only possible for the Newtonian case. The governing equation for the Newtonian case *without axial conduction* assumes the following form:

$$S''(\bar{r}) + \frac{1}{\bar{r}} S'(\bar{r}) + \lambda_n^2 [1 - \bar{r}^2] S(\bar{r}) = 0 \quad (27)$$

This is the classical equation obtained by Graetz for determination of the eigenfunction in the case of Poiseuille flow of a Newtonian fluid through a circular duct. The solution of Eqn. (26) can be obtained via an appropriate numerical technique [31] or by converting it into a confluent hypergeometric equation [32]. Another approach is to use the *power-series* method. Accordingly, we assume the solution of Eqn. (27) in the form:

$$S = \sum_{j=0}^{\infty} E_j \bar{r}^j \quad (28)$$

Now taking the derivative of the above equation and then plugging into the original Eqn. (27), one can obtain:

$$\left. \begin{aligned} &2E_2 + 3.2E_3\bar{r} + \dots + (j+2)(j+1)E_{j+2}\bar{r}^j + \frac{E_1}{\bar{r}} + 2E_2 + 3E_3\bar{r} + \dots \\ &+ (j+1)E_{j+1}\bar{r}^{j-1} + (j+2)E_{j+2}\bar{r}^j + \lambda^2 E_0 + \lambda^2 E_2\bar{r} + \lambda^2 E_2\bar{r}^2 + \dots + \lambda^2 E_j\bar{r}^j \\ &= \lambda^2 E_0\bar{r}^2 + \lambda^2 E_1\bar{r}^3 + \lambda^2 E_2\bar{r}^4 + \dots + \lambda^2 E_n\bar{r}^{j+2} \end{aligned} \right\} \quad (29)$$

Equating the powers of \bar{r} on both sides of Eqn. (29) yields the following hierarchy of equations:

$$\left. \begin{aligned} &E_1 = 0 \\ &2.1E_2 + 2E_2 + \lambda^2 E_0 = 0 \\ &3.2E_3 + 3E_3 + \lambda^2 E_1 = 0 \\ &4.3E_4 + 4E_4 + \lambda^2 E_2 = \lambda^2 E_0 \\ &5.4E_5 + 5E_5 + \lambda^2 E_3 = \lambda^2 E_1 \\ &\dots \quad \dots \quad \dots \quad \dots \quad \dots \quad \dots \\ &\dots \quad \dots \quad \dots \quad \dots \quad \dots \quad \dots \end{aligned} \right\} \quad (30)$$

and so on.

In general, the coefficients E_n satisfy the relation:

$$(j+2)(j+1)E_{j+2} + (j+2)E_{j+2} + \lambda^2 E_j = \lambda^2 E_{j-2} \quad \text{for } j \geq 2 \quad (31)$$

Note that *all odd coefficients* are zero since $E_1 = 0$. Substituting $j = 2m$ in Eqn. (31) yields the following recurrence relation for *even* coefficients.

$$E_{2m} = \frac{\lambda^2}{(2m)^2} (E_{2m-4} - E_{2m-2}) \quad (32)$$

Therefore, we can write:

$$S = \sum_{j=0}^{\infty} E_{2j} \bar{r}^{2j}, \quad (33)$$

Here:

$$E_{2j} = \frac{\lambda^2}{(2j)^2} [E_{2j-4} - E_{2j-2}] \text{ for } j \geq 2. \quad (34)$$

Expanding Eqn. (32), one may write:

$$S = E_0 + E_2 \bar{r}^2 + E_4 \bar{r}^4 + \dots \quad (35)$$

The boundary condition $S'(0) = 0$ is automatically satisfied while the auxiliary condition $S(0) = 1$ gives $E_0 = 1$. Employing the remaining boundary condition $S(1) = 0$ and retaining the first five terms in the above series yields the following equation for determination of the first four eigenvalues:

$$\lambda^4 - 27\lambda^2 + 144 = 0 \quad (36)$$

Table 1: Comparison of the first four eigenvalues computed with both numerical and analytical approaches

λ_n	Analytical results (series solution)	Analytical results (Kummer function approach) [25]	Numerical results (Bvp5c)
λ_1	2.70436	2.70436	2.70436
λ_2	6.6790	6.6790	6.6790
λ_3	10.6734	10.6734	10.6734
λ_4	14.6711	14.6711	14.6711

The solution of Eqn. (35) obtained via the Newton-Raphson method for eigenvalues is depicted in **Table 1**. Now in order to check the accuracy of the numerical approach Eqn. (20) is solved

with the aid of Matlab software (Bvp5c) for the Newtonian case with negligible axial conduction. **Appendix 2** gives some details on the Bvp5c algorithm. The eigenvalues obtained are listed in third column of **Table 1**. For completeness the eigenvalues obtained via the Kummer function approach [32] are also listed in column two of **Table 1**. A perfect match is observed in all the three cases. This corroborates the Bvp5c approach and therefore, one can confidently apply this numerical scheme for further analysis and capture the non-Newtonian effect in this classical problem of fluid dynamics.

3.1 Experimental validation

Before advancing towards the numerical and graphical results of the considered problem, it is judicious to validate the numerical results, where possible, with available experimental data. For this purpose, we compare the numerical results for fully developed Nusselt numbers with $\beta^*=0.0001$ and $q=-1$ with the experimental data for fully developed Nusselt numbers for the classical Graetz problem in a tube as illustrated in Figure 1(b). Inspection of the graph reveals that the theoretical results achieve excellent agreement with the experimental observations reported in Hemadria *et al.* [33] for all axial locations in the tube.

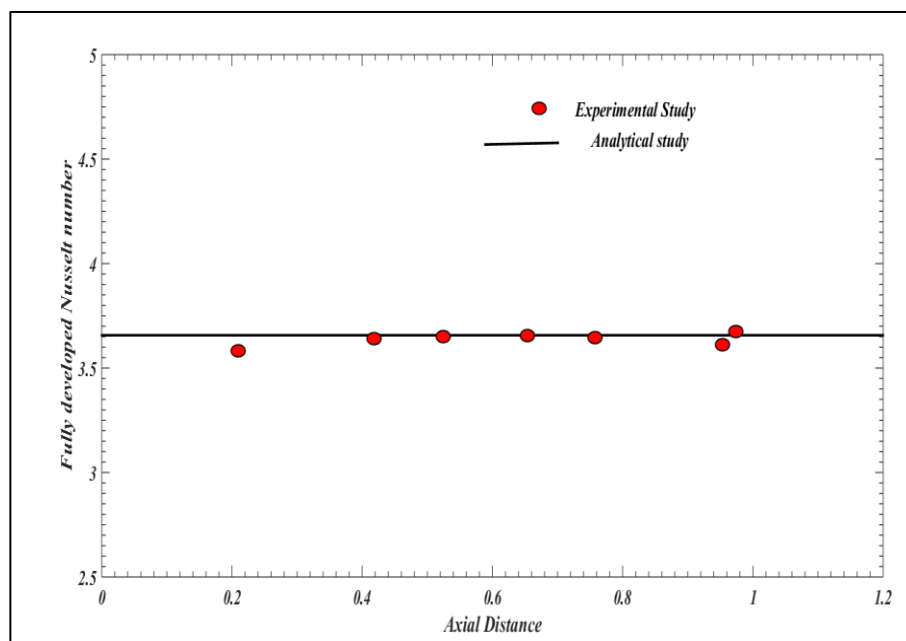


Figure 1(b): Experimental validation of local Nusselt number with axial distance

4. Results and Discussion

The Graetz problem is elaborated for Quemada bio-rheological fluid by solving the energy equation based on Fourier's law (Eqn. (3)) with the help of the method of separation of

variables. A complete analytical solution is not possible due to the non-availability of the exact solution of Eqn. (20). Therefore, the eigenvalues and eigenfunctions associated with Eqn. (20) are computed with the Matlab built-in solver, Bvp5c [See **Appendix 2**]. The coefficient of solution series in Eqn. (22) are computed through numerical integration. The solution $\theta(\bar{r}, \bar{z})$ thus obtained is further employed in the evaluation of the average temperature and Nusselt numbers. The relevant literature – see Victor and Shah [34]- shows that the typical value of Prandtl number for streaming blood is 25. Additional properties of blood are reported in **Table 2**. Therefore, all our analysis is carried out for $Pr = 25$. On the basis of the information reported in **Table 2** the plausible ranges for Reynolds number and Péclet number for the core vascular, subcutaneous vascular and microvascular regions are given in **Table 3**.

Table 2: Properties of blood [34]

<i>Value</i>	<i>Physiological Solution</i>
Specific heat	
0.94 cal/g °C	Plasma
0.77	RBC
0.87	Plasma and RBC
0.92	Whole blood
0.94	Plasma
Relative viscosity (ratio to water)	
3.54.0	Whole blood
2.54.0	Whole blood
4.71	Whole blood at 20°C
3.00	Whole blood at 37°C
1.32-1.22	Plasma
3.5-5.4	Whole blood
Apparent viscosity	
0.012 P	Plasma
0.035 P	Whole blood
Thermal conductivity	
0.5 w/m °K	Whole blood
0.506 w/m °K	Whole blood
0.582 w/m °K	Plasma
0.48 1 w/m °K	Corpuscles
1.365 Cal/cm s °C * 10 ³	Plasma
1.265 Cal/cm s °C * 10 ³	Blood 43%, hemocrit

Table 3: Reynolds and Péclet number ranges for blood

Blood vessel region	Reynolds number	Péclet number
Core vascular	100-1000	2500-25000
Subcutaneous vascular	1-10	25-250
Microvascular	0.001	0.025

4.1 Physical significance

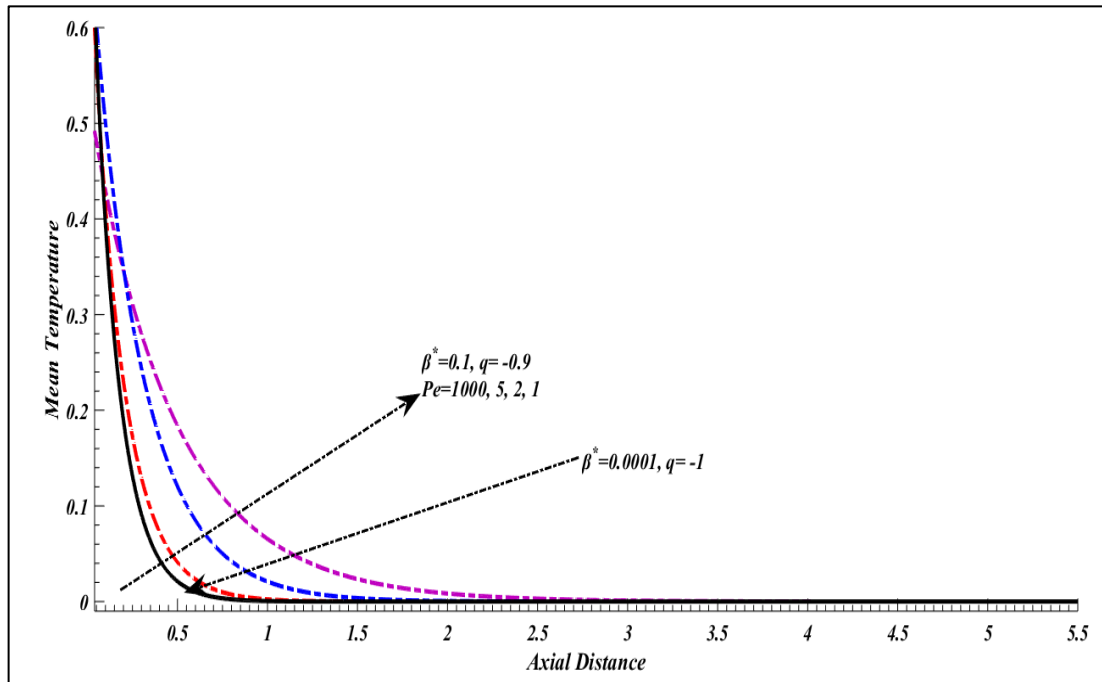


Figure 2: Mean temperature for various values of Péclet number in the presence of Quemada parameters

Consider a tube having an insulated region confined to the *upstream domain* $\bar{z} < 0$, followed by a region of heat transfer in the *downstream domain* $\bar{z} > 0$. A significant amount of heat transfer is expected between these two regions due to axial conduction in the fluid via the cross-section at axial station $\bar{z} = 0$ for low Péclet numbers. Therefore, the temperature of the fluid flowing through the heat transfer region is *unknown* i.e., to be computed. The present model assumes that the fluid inlet temperature is T_i and inlet axial location is sufficiently far away from the cross-section at $\bar{z} = 0$ from where the region of the applied heat transfer begins. The boundary condition implies that at the start of the heat transfer region $\bar{z} = 0$ there is a *sudden change* in the wall temperature from T_i to T_s . The above model may also find applications in thermoregulation of blood via thermal biomedical devices such as blood temperature monitors

[35, 36] used in dialysis and cancer treatment where hypovolaemia, hyperthermia (excessive heat removal due to reduced vascular resistance which increases blood perfusion in the capillary regions of the skin), hypothermia (excessive heat release due to increased peripheral resistance which reduces blood perfusion in the capillary regions of the skin) are key considerations. The sustaining of a comfortable core body temperature is therefore achieved via thermoregulation. In particular the thermoregulation of blood is strongly influenced by viscosity which is in turn influenced by rheology [36]. For more accurate predictions of actual blood thermal characteristics therefore a good *non-Newtonian* model is essential.

4.2 Mean temperature

Figure 2 and 3 depict the influence of Péclet number on the mean temperature in the presence of Quemada parameters under uniform wall temperature boundary condition. As expected, the influence of Péclet number is strongly pronounced near the thermal entrance region – here decreasing the Péclet number results in *higher mean temperatures*. Further, the mean temperature is higher for microvascular region in comparison with subcutaneous vascular and core vascular regions. It is also observed that mean temperature decreases gradually and approaches to zero in the downstream region. Thus, axial conduction delays the prevalence of fully developed conditions in the downstream region. **Figure 4** displays the behaviour of temperature gradient for various values of Péclet numbers in the presence of Quemada parameters. Temperature gradient exhibits similar trend with respect to Péclet number which has been observed for mean temperature. However, the temperature gradient curves are much steeper than the corresponding curves of mean temperature and that is why they achieve the fully developed conditions in the vicinity of the entrance region.

4.3 Local Nusselt number

Figure 5 shows the behaviour of local Nusselt number for various values of Péclet number for three regions namely, microvascular, subcutaneous and core regions under the influence of Quemada parameters. It is emphasized that local Nusselt number *in the microvascular region* for the fully developed case is *higher* than the corresponding Nusselt numbers in fully developed case for subcutaneous and core regions. This is expected since Péclet number in microvascular region is substantially lower than the Péclet number in *subcutaneous vascular* and *core vascular* regions. As a result, greater heat transfer is expected in micro vessels resulting in a *higher* fully developed Nusselt number.

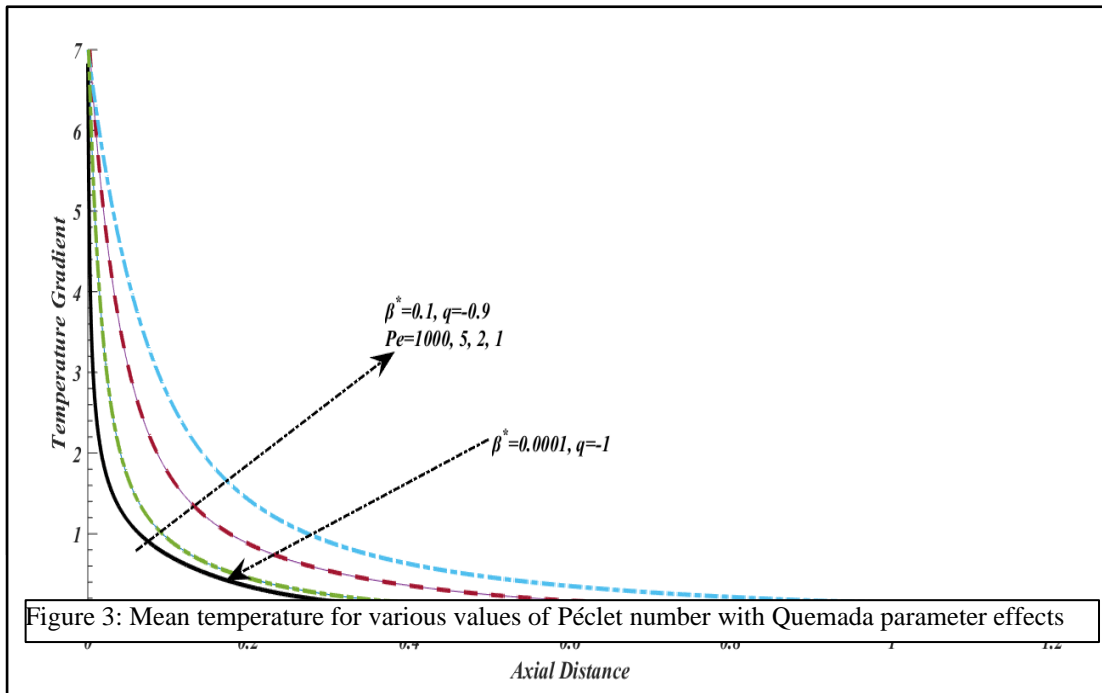


Figure 4: Temperature gradient for various values of Péclet numbers

Figure 6 displays the variation of local Nusselt number at $Pe = 1$ for different values of Quemada parameters. *Péclet number* expresses the ratio of the rate of advection of a physical quantity by the flow to the rate of diffusion (e. g. species or heat). For the value of unity considered both momentum advection rate and heat diffusion rate are equal. It is apparent that local Nusselt number is higher for greater values of Quemada parameters i. e. stronger rheological effects. The effects are more pronounced in the entrance region and they gradually diminish with advancement toward the downstream region. Nevertheless, though diminishing, these effects still manifest themselves in the form of higher local Nusselt number in the fully developed region. It is important to mention that both parameters β^* and q characterize the shear-thinning (pseudoplastic) nature of the fluid. In this context, it may be concluded that shear-thinning character of the fluid results in the enhancement of local Nusselt number from its Newtonian value in both entrance and fully developed regions. Blood rheology therefore clearly strongly influences heat transfer behaviour [37, 38].

Figure 7 presents the comparison between the local Nusselt number for Newtonian fluid without axial conduction and the local Nusselt number for Quemada fluid (blood) with strong

axial conduction effect at different axial locations. It is apparent that local Nusselt number for Quemada fluid model *with longitudinal conduction* attains higher numerical values than the corresponding Nusselt number for Newtonian fluid with *no axial conduction* effect. From the proceeding discussion, it may be concluded that *both mean temperature and local Nusselt number are highly sensitive* to Péclet number and Quemada parameters. In facts, both of these parameters significantly influence the heat transfer in the thermal entrance region of the circular tube.

Table 4 represents the numerical values for fully developed local Nusselt number for different values of Péclet number for both Newtonian and Quemada fluids. Again, it is clearly seen that fully developed local Nusselt number achieves higher numerical values for smaller values of Péclet number. In addition, it is shown that the numerical values of fully developed local Nusselt number for shear-thinning Quemada fluid are *higher* than their counterparts for Newtonian model. Thus shear-thinning characteristics enhance the heat transfer in *both thermal entrance and fully developed regions*.

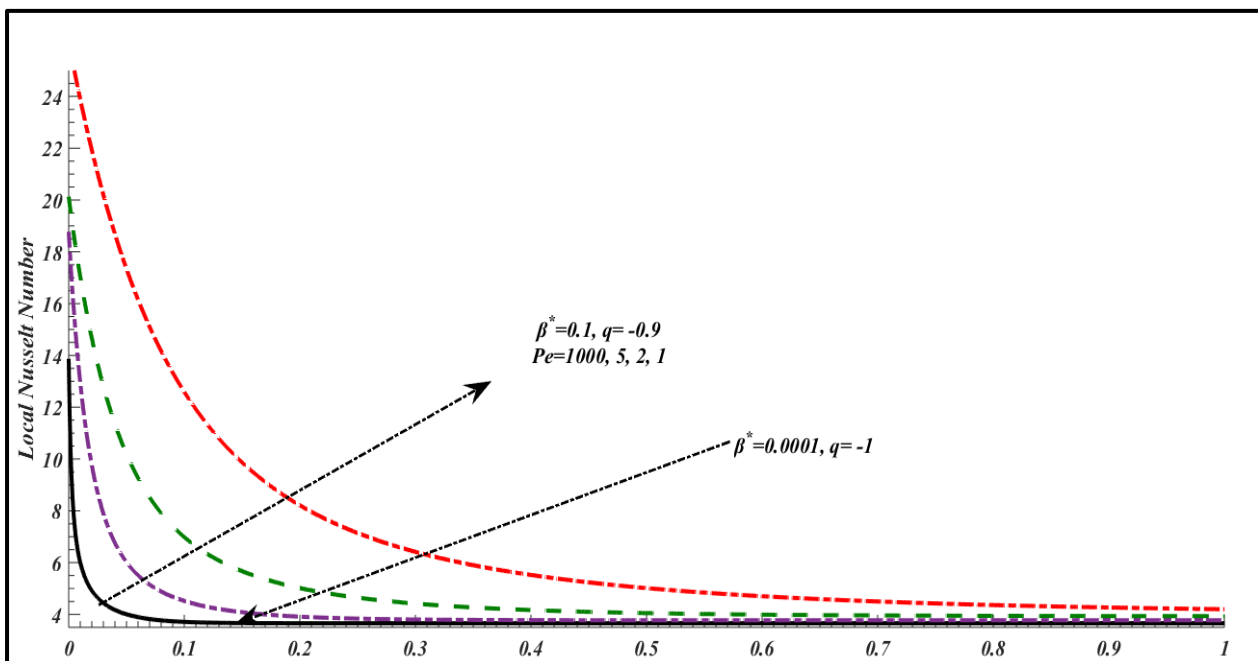


Figure 5: Local Nusselt number for various values of Péclet number in the presence of Quemada parameters

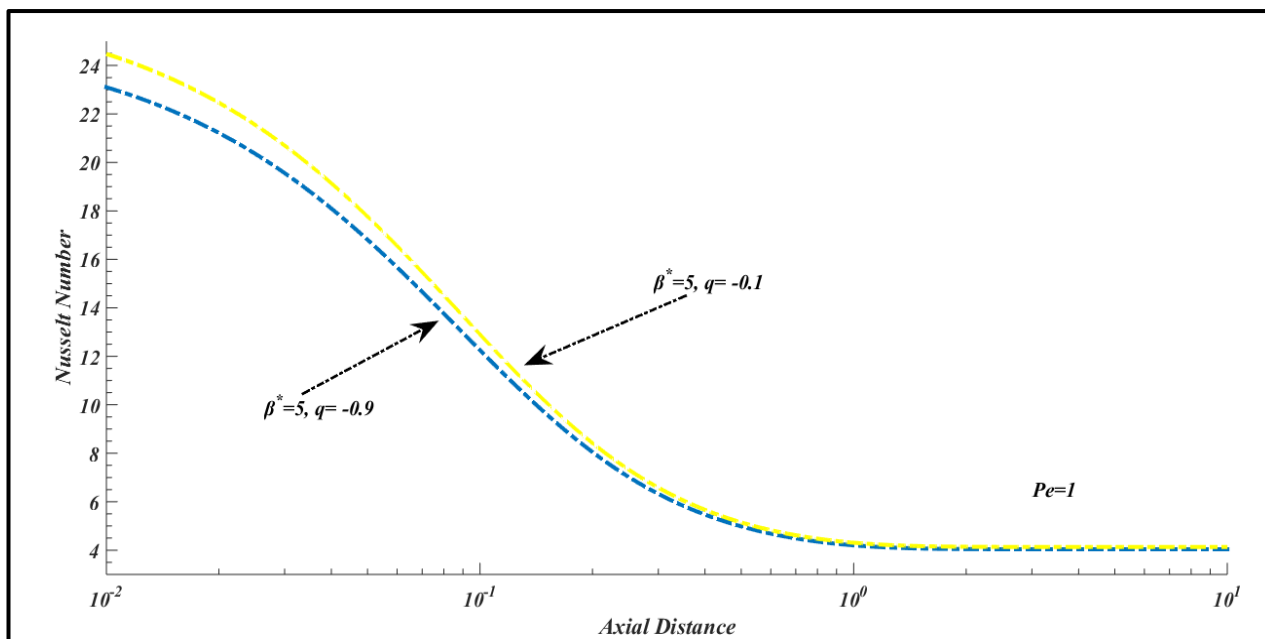


Figure 6: Local Nusselt number for various values of Quemada parameters at $Pe = 1$

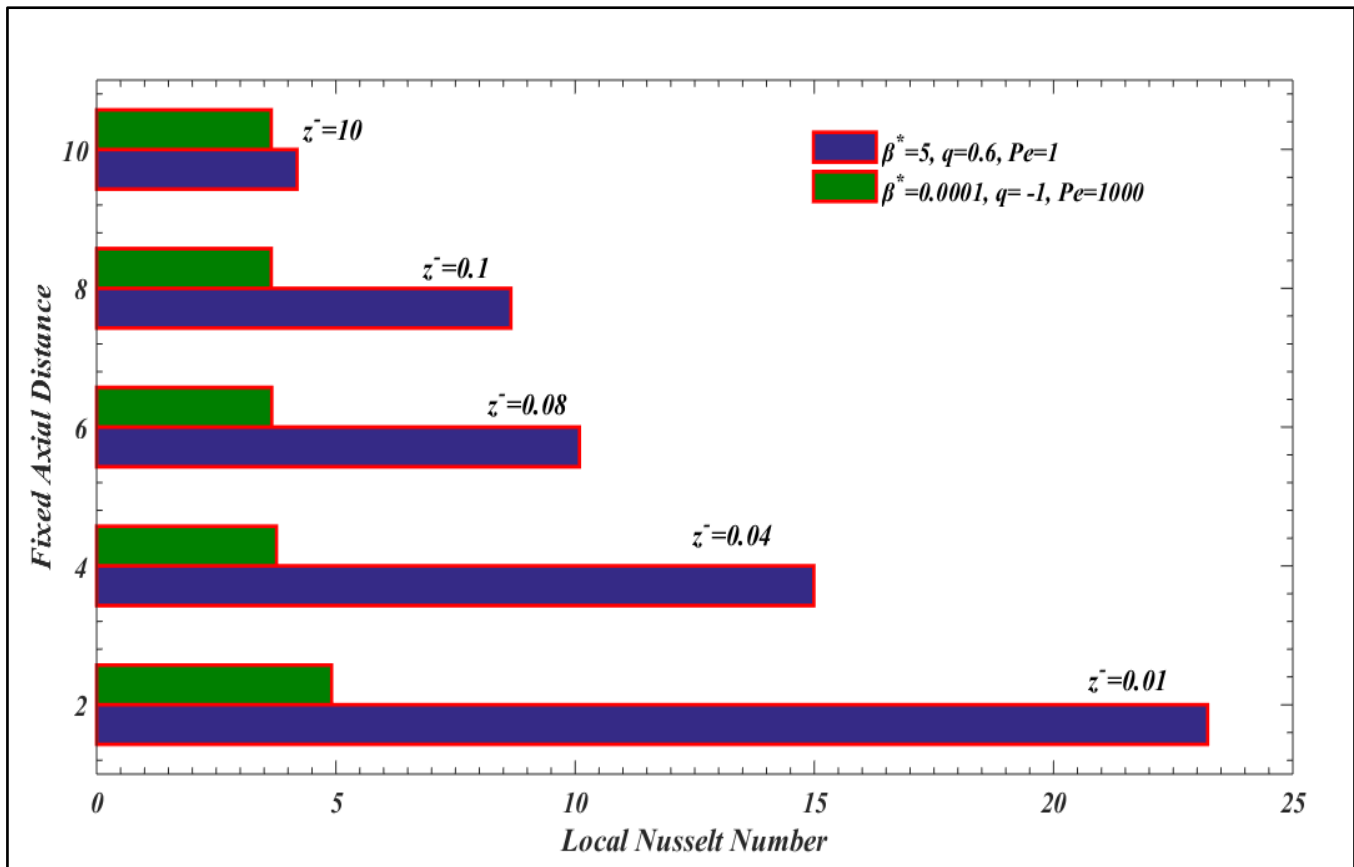


Figure 7: Local Nusselt number for various values of Quemada parameters

Table 4 Numerical values of fully developed local Nusselt number for different values of Quemada parameters and Péclet numbers.

Pe	$Nu(\bar{z})$	
	$(\beta^* = 0.0001, q = -1)$	$(\beta^* = 5, q = -0.1)$
1000	3.657	3.67
10	3.67	3.84
5	3.76	3.96
3	3.85	4.03
1	4.03	4.13
0.7	4.07	4.15
0.1	4.167	4.18
0.025	4.17	4.21
0.001	4.182	-

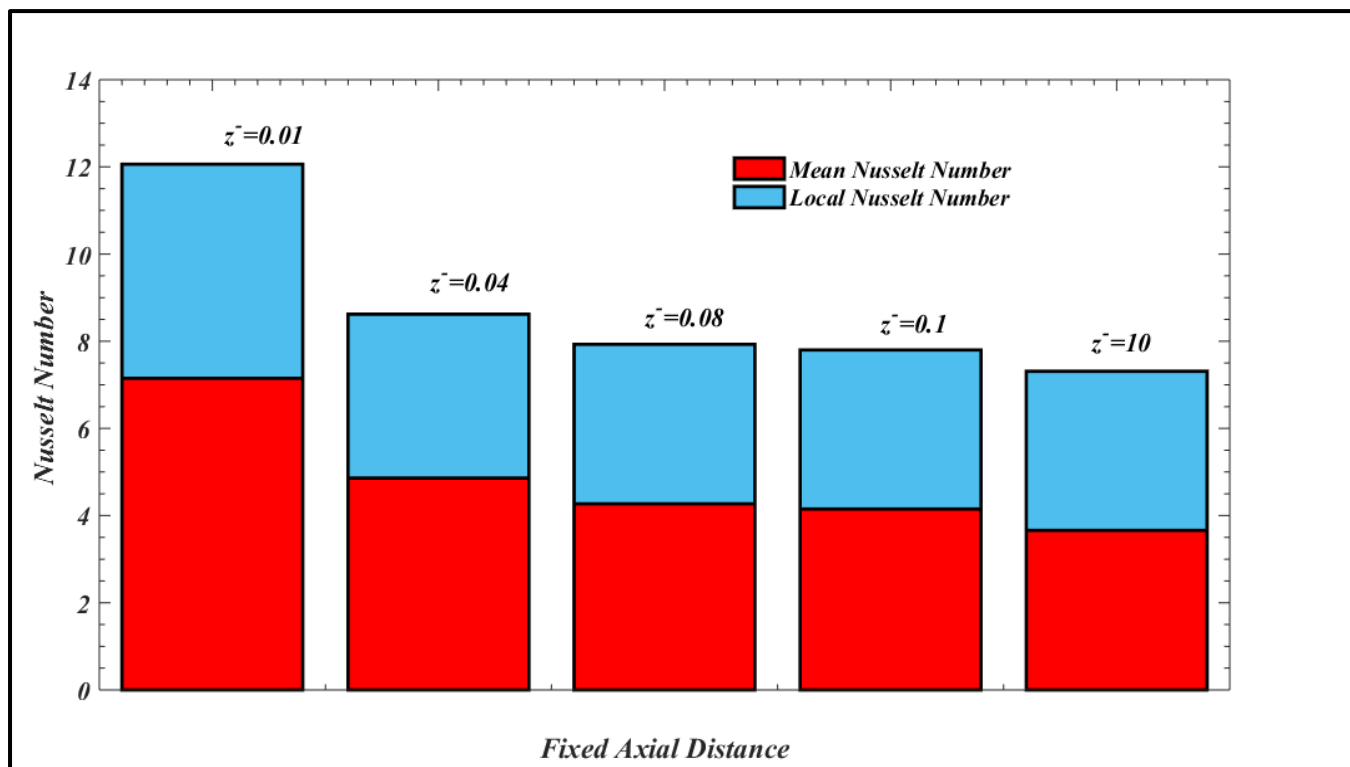


Figure 8: Local and Mean Nusselt number at $Pe = 1000$ and $\beta^* = 0.0001$, $q = -1$

Lastly, **Figure 8** depicts both local and mean Nusselt numbers at different axial location for Quemada parameters corresponding to the Newtonian case. As expected, *mean* Nusselt number is higher in comparison with *local* Nusselt number at each axial station. A further increase in both local and mean Nusselt numbers is anticipated with an increase in the Quemada parameters.

5. Conclusions

In the present investigation the classical Graetz problem has been extended for Quemada bio-rheological fluid model. The two-dimensional energy equation is tackled via the method of separation of variables. The Matlab solver Bvp5c is used to compute numerical solution of the eigenvalue problem. Coefficients of solution series are computed via numerical integration. Numerical validation is presented with a power series solution and via benchmarking with available exact solutions in the literature. To provide an insight into the mathematical relevance of the mathematical model to clinical situations involving heat transfer in blood flows (for e.g. thermoregulation devices), the results for mean temperature and local Nusselt number are

presented based on the data of Péclet number for blood in different regimes. In particular, the influence of Péclet number on mean temperature and local Nusselt number for three vascular regions namely, core vascular, subcutaneous vascular and microvascular regions is thoroughly studied. The following observations are made.

- Enhancing the shear-thinning nature of the Quemada fluid increases the local Nusselt number.
- Local Nusselt number increases for the smaller values of Péclet number.
- Fully developed Nusselt number is an increasing function of the Quemada rheological model parameters.
- Mean Nusselt number is always higher than local Nusselt number under similar conditions.
- Mean temperature distribution significantly depends on Péclet number and it achieves higher values in thermal entrance region for lower Péclet numbers.
- Péclet number has a strong impact in microvascular region as compared with subcutaneous vascular.
- Core vascular region is almost independent of Péclet number.
- For both microvascular and subcutaneous regions, the fully developed condition is acquired earlier either by raising the Péclet number or by tuning the properties of Quemada fluid model.
- In the core vascular region, the fully developed condition can be attained earlier only by tuning the mechanical properties of the non-Newtonian Quemada fluid.

References

- [1] M. Bureau, J. Healy, D. Bourgoïn and M. Joly, Etude Experimentale, In Vitro du Comportement Rheologie du Sang et Regime Transitoire a Faible Vitessed e Cisaillement, *Rheol. Acta*, **17**,612-625(1978).
- [2] M. Bureau, J. Healy, D. Bourgoïn and M. Joly, Rheological Hysteresis of Blood at Low Shear Rate, *Biorheology*, **17**,191-203(1980).
- [3] G. W. Burgreen, J. F. I. Antak, Z. J. Wu and A. J. Holmes, Computational Fluid Dynamics as a Development Tool for Rotary Blood Pumps, *Artif Organs*, **25(5)**, 336-340(2001).
- [4] L. Graetz, Über die Wärmeleitungsfähigkeit von Flüssigkeiten, part 1. *Annalen der Physik und Chemie*, **18**, 79-94 (1883); part 2, **25**, 337-357 (1885).
- [5] W. Nusselt, Die abhângigkeit der wärmeübergangszahl von der rohrlänge (The dependence of the heat transfer coefficient on the tube length), *Z. ver. Deut. Ing.* **54**, 1154–1158(1910).
- [6] R. Siegel, E. M. Sparrow and T. M. Hallman, Steady laminar heat transfer in a circular tube with prescribed wall heat flux, *Appl. Sci. Res.*, **7**, 386-392 (1958).
- [7] C. J. Hsu, “Theoretical solutions for low-Peclet-number thermal-entry-region heat transfer in laminar flow through concentric annuli”, *Int. J. Heat Mass Tran.* **13**, 1907–1924 (1970).
- [8] C. J. Hsu, An Exact Mathematical Solution for Entrance Region Laminar Heat Transfer with Axial Conduction, *Appl. Sci. Res.*, **17**, 359(1967).
- [9] C. J. Hsu, Exact solution to entry-region laminar heat transfer with axial conduction and the boundary condition of the third kind, *Chem. Eng. Sci.*, **23**, 457(1968).
- [10] R. K. Shah and A. L. London, “Laminar flow forced convection in ducts”, 3rd. Ed., academic press, New York (1978).
- [11] P. R. Johnston, Axial conduction and the Graetz problem for a Bingham plastic in laminar tube flow, *Int. J. Heat Mass Transfer*, **34**, 1209–1217 (1991).
- [12] P. R. Johnston, A Solution Method for the Graetz Problem for Non-Newtonian Fluids with Dirichlet and Neumann Boundary Conditions, *Math. Comp. Modelling*, **19**, 1-19 (1994).
- [13] J. Lahjomri and A. Quabarra, Analytical solution of the Graetz problem with axial conduction, *J. Heat Tran.* **121**, 1078–1083 (1999).

- [14] P. M. Coelho, F. T. Pinho and P. J. Oliveira, “Thermal entry flow for a viscoelastic fluid, The Graetz problem for the PTT model”, *Int. J. Heat Mass Tran.*, **46**, 3865–3880 (2003).
- [15] P. J. Oliveira, P. M. Coelho and F. T. Pinho, The Graetz problem with viscous dissipation for FENE-P fluids, *J. Non-Newtonian Fluid Mech.*, **121**, 69–72(2004).
- [16] A. Filali, L. Khezzar, D. Siginer and Z. Nemouchi, Graetz problem with non-linear viscoelastic fluids in non-circular tubes, *Int. J. Thermal Sci.*, **61**, 50e60(2012).
- [17] N. Ali and M. W. S. Khan, The Graetz problem for the Ellis fluid model, *Zeitschrift für Naturforschung A (ZNA)*, **74**, 15-24 (2019).
- [18] M. W. S. Khan and N. Ali, Theoretical analysis of thermal entrance problem for blood flow: An extension of classical Graetz problem for Casson fluid model using generalized orthogonality relations, *Int. Commun. Heat Mass* **108**, 104314 (2019).
- [19] M. W. S. Khan, N. Ali and Z. Asghar, Thermal and rheological effects in a classical Graetz problem using a nonlinear Robertson-Stiff fluid model. *Heat Tran.* 1–18. <https://doi.org/10.1002/htj.21980>, (2020).
- [20] D. Quemada, Rheology of concentrated dispersed systems: II. A model for non-Newtonian shear viscosity in shear flows, *Rheol. Acta*, **17**,632-642 (1978a).
- [21] B. Das, G.. Enden and A. S. Popel, Stratified multiphase model for blood flow in a venular bifurcation, *Annals of Biomedical Engineering*. 25 (1997), 135–153.
- [22] Sriram K. *et al.*, Non-Newtonian flow of blood in arterioles: consequences for wall shear stress measurements., *Microcirculation*, 21(7):628-639 (2014).
- [23] Marcinkowska-Gapinska A, Gapinski J, Elikowski W, Jaroszyk F, Kubisz L. Comparison of three rheological models of shear flow behavior studied on blood samples from post-infarction patients. *Med. Bio. Eng. Comput.* 2007; 45: 837–844.
- [24] Adrian Postelnicu *et al.*, Steady flow in the Willis circle using a Quemada model, 7 (1), *Sixth International Congress on Industrial Applied Mathematics (ICIAM07) and GAMM Annual Meeting, Zürich 2007*, December (2007).
- [25] P. Naeofytou, Comparison of blood rheological models for physiological flow simulation, *Biorheology*, vol. 41, no. 6, pp. 693-714 (2004).
- [26] P. L. Easthope and D. E. Brooks, A comparison of rheological constitutive functions for whole human blood, *Biorheology*, **17**, 235 - 247(1980).
- [27] A. S. Popel and G. Enden, An analytical solution for steady flow of a Quemada fluid in a circular tube, *Rheol. Acta*, **12**, 422-42 (1993).

- [28] E. Kreyzig, *Advanced Engineering Mathematics*, 9th edn, Wiley, New York (2006).
- [29] A. H. Sheikh, J. V. Beck and D. E. Amos, Axial heat conduction effects in the entrance region of parallel plate ducts. *Int. J Heat Mass Tran.*, **51**, 5811–5822(2008).
- [30] J. Lahjomri, A. Quabarra and A. Alemany, Heat transfer by laminar Hartmann flow in thermal entrance region with a step change in wall temperatures: the Graetz problem extended, *Int. J. Heat Mass Tran.*, **45**, 1127–1148(2002).
- [31] M. D. Mikhailov and R. M. Cotta, Eigenvalues for the Graetz problem in slip-flow, *Int. Comm. Heat Mass*, **24**, 449 (1997).
- [32] V. Hemadria, G.S. Biradarb, N. Shahc, R. Garga, U. V. Bhandarkara and A. Agrawa, Experimental study of heat transfer in rarefied gas flow in a circular tube with constant wall temperature, *Exp. Therm. Fluid Sci.*, **93**, 326-33(2018).
- [33] S. A. Victor and V. L. Shah, Steady state heat transfer to blood flowing in the entrance region of a tube, *Int. J. Heat Mass Tran.*, **19**, 777–783(1976).
- [34] A. Shitzer and R. C. Eberhart (eds.), *Heat Transfer in Medicine and Biology*, Plenum, New York, Vol. II (1985).
- [35] Mashour GA, Boock RJ. Effects of shear stress on nitric oxide levels of human cerebral endothelial cells cultured in an artificial capillary system. *Brain Res.* 1999; 842(1):233–238.
- [36] Quemada D., (1983) Blood rheology and its implications in flow of blood. In: *Rodkiewicz CM (ed) Arteries and arterial blood flow*. Biological and physiological aspects. Springer Verlag, New York, pp 1–127.
- [37] Popel A.S., Johnson P.C., Microcirculation and hemorheology. *Ann. Rev. Fluid Mech.* 2005; 37:43–69.

Appendix 1: Coefficients in polynomials in terms of q

$$\begin{aligned}
A_1 &= \frac{-1}{7}(q+8) \\
A_2 &= \frac{-1}{42}(13q^2 - 8q - 7) \\
A_3 &= \frac{-1}{210}(143q^3 - 88q^2 - 113q + 48) \\
A_4 &= \frac{-1}{840}(1287q^4 - 792q^3 - 1342q^2 + 632q + 175) \\
A_5 &= \frac{-1}{840}(3003q^5 - 1848q^4 - 3894q^3 + 1944q^2 + 1011q - 256) \\
A_6 &= \frac{-1}{1680}(15015q^6 - 9240q^5 - 23331q^4 + 12096q^3 + 9081q^2 - 3176q - 525) \\
A_7 &= \frac{-1}{1680}(45045q^7 - 27720q^6 - 82005q^5 + 43680q^4 - 42819q^3 - 17304q^2 - 5619q + 1024) \\
A_8 &= \frac{-1}{16}(1-q)^2(1+q)(429q^5 + 165q^4 - 330q^3 - 90q^2 + 45q + 5)
\end{aligned} \tag{A1}$$

Appendix 2: MATLAB bvp5c solver

The MATLAB bvp5c solver is a superior algorithm to the more customary bvp4c solver, and directly controls the true error in the calculation, while bvp4c controls it only indirectly. At more stringent error tolerances, this difference between the solvers is not as apparent as noted by Shampine and Kierzenka [A1]. bvp5c is a finite difference code that implements the four-stage Lobatto IIIa formula which is a collocation formula and the collocation polynomial provides a C^1 -continuous solution that is fifth-order accurate uniformly in [a,b]. The formula is implemented as an implicit Runge-Kutta formula. bvp5c does not utilize analytical condensation which is present in bvp4c. Unlike bvp4c which handles unknown parameters directly, bvp5c augments the system with trivial differential equations for the unknown parameters. For robustness the new solver is based on control of a residual. The residual is scaled so that it has the same order of convergence as the true error. For a large class of methods, bvp5c [A2] has been verified to confirm that if this scaled residual is less than a given tolerance, then asymptotically the true error is also less than the tolerance. Bvp5c interpolates the value and gradient at both ends of the subinterval and the value of y_{mid} at the midpoint. The following stepping formula is used as elaborated by Russel and Christansen [A3]:

$$Y_{MID} = Y_1 + \zeta \left[\frac{17}{192}K_1 + \frac{40+15\sqrt{5}}{192}K_2 + \frac{40-15\sqrt{5}}{192}K_3 - \frac{1}{192}K_4 \right] \tag{A2}$$

Here Y_I is the initial guess and K_1, K_2, K_3, K_4 are the approximations with a stepping distance of ζ . The algorithm is very efficient, unconditionally stable and produces excellent accuracy with fast compilation times.

Supplementary References

[A1] Shampine, L.F., and J. Kierzenka, A BVP solver that controls residual and error (MATLAB bvp5c), *J. Numer. Anal. Ind. Appl. Math.* 3(1/2), 27–41 (2008).

[A2] S. Pal, *Numerical Methods: Principles, Analyses and Algorithms*, Oxford University Press, India (2009).

[A3] R.D. Russell and J. Christiansen, Adaptive mesh selection strategies for solving boundary value problems, *SIAM J. Numer. Anal.*, 14, 59–80 (1978).
